Journal of Biotechnology 169 (2014) 23–33

Contents lists available at ScienceDirect

Journal of Biotechnology

journal homepage: www.elsevier.com/locate/jbiotec

Molecular characterization of an aldo-keto reductase from *Marivirga tractuosa* that converts retinal to retinol

Seung-Hye Hong[a,1], Hyun-Koo Nam[a,1], Kyoung-Rok Kim[a], Seon-Won Kim[b], Deok-Kun Oh[a,*]

[a] Department of Bioscience and Biotechnology, Konkuk University, Seoul 143-701, Republic of Korea
[b] Division of Applied Life Science, EB-NCRC and PMBBRC, Gyeongsang National University, Jinju 660-701, Republic of Korea

ARTICLE INFO

Article history:
Received 13 August 2013
Received in revised form 10 October 2013
Accepted 11 November 2013
Available online 20 November 2013

Keywords:
Aldo-keto reductase
Cofactor-binding residues
Marivirga tractuosa
Retinal
Retinol

ABSTRACT

A recombinant aldo-keto reductase (AKR) from *Marivirga tractuosa* was purified with a specific activity of 0.32 unit ml^{-1} for all-*trans*-retinal with a 72 kDa dimer. The enzyme had substrate specificity for aldehydes but not for alcohols, carbonyls, or monosaccharides. The enzyme turnover was the highest for benzaldehyde (k_{cat} = 446 min^{-1}), whereas the affinity and catalytic efficiency were the highest for all-*trans*-retinal (K_m = 48 μM, k_{cat}/K_m = 427 mM^{-1} min^{-1}) among the tested substrates. The optimal reaction conditions for the production of all-*trans*-retinol from all-*trans*-retinal by *M. tractuosa* AKR were pH 7.5, 30 °C, 5% (v/v) methanol, 1% (w/v) hydroquinone, 10 mM NADPH, 1710 mg l^{-1} all-*trans*-retinal, and 3 unit ml^{-1} enzyme. Under these optimized conditions, the enzyme produced 1090 mg ml^{-1} all-*trans*-retinol, with a conversion yield of 64% (w/w) and a volumetric productivity of 818 mg l^{-1} h^{-1}. AKR from *M. tractuosa* showed no activity for all-*trans*-retinol using $NADP^+$ as a cofactor, whereas human AKR exhibited activity. When the cofactor-binding residues (Ala158, Lys212, and Gln270) of *M. tractuosa* AKR were changed to the corresponding residues of human AKR (Ser160, Pro212, and Glu272), the A158S and Q270E variants exhibited activity for all-*trans*-retinol. Thus, amino acids at positions 158 and 270 of *M. tractuosa* AKR are determinant residues of the activity for all-*trans*-retinol.

1. Introduction

Retinoids have been extensively studied over the last decades (Blomhoff and Blomhoff, 2006). Retinoids include retinal, retinol, retinoic acid, and retinyl ester, which are the aldehyde, alcohol, oxidized, and ester forms of vitamin A, respectively, and they participate in growth (Raifen et al., 1996), immune system (Mora et al., 2008), vision (von Lintig, 2012), and gene signaling (Pino-Lagos et al., 2010).

Commercial retinol production is currently conducted *via* chemical synthesis through the acid or base reduction of a pentadiene derivative followed by the acidification/hydrolysis of the isomeric mixture to generate retinol (Mercier and Chabardes, 1994). Although this chemical process is economic, the method has some disadvantages, including complex purification steps, the formation of chemical wastes, and the formation of undesired by-products. Moreover, the product of the chemical process is not retinol but retinol acetate. Thus, the biological manufacture of retinol has been focused in recent years (Kim and Oh, 2010).

The enzymes catalyzing the oxidation and reduction of retinal are classified into 4 distinct types: alcohol dehydrogenases (ADHs) of the medium-chain dehydrogenase (MDR) family, short-chain dehydrogenase (SDR), the aldehyde dehydrogenase (ALDH), and aldo-keto reductase (AKR) families (Duester et al., 2003). ADHs, SDRs and AKRs oxidize retinol to retinal and reduce retinal to retinol, whereas ALDHs oxidize retinal to retinoic acid. SDRs and AKRs prefer $NADP^+$/NADPH over NAD^+/NADH and catalyze the reverse reaction, reduction of retinal to retinol which can then be esterified and stored as retinyl esters (Ruiz et al., 2012). ADHs also catalyze the reversible reaction but prefer NAD^+/NADH to $NADP^+$/NADPH (Duester, 1996). In contrast, ALDHs catalyze the irreversible oxidation of retinal to retinoic acid.

AKR family (EC 1.1.1.21) includes a number of NADPH-dependent oxidoreductases, such as aldehyde reductase, aldose reductase, prostaglandin F synthase, xylose reductase, rho crystallin, and many other enzymes (Bohren et al., 1989). The activity of AKR for retinal as a substrate has been reported in the subfamily 1B (aldose reductase) and 1C (prostaglandin F synthase), including AKR1B1, AKR1B10, and AKR1B12 from human, AKR1C7 from chicken, and AKR1C15 from rat (Crosas et al., 2001; Duester, 2000;

* Corresponding author. Tel.: +82 2 454 3118; fax: +82 2 444 5518.
E-mail address: deokkun@konkuk.ac.kr (D.-K. Oh).
[1] These authors equally contributed to this paper.

0168-1656/$ – see front matter.
http://dx.doi.org/10.1016/j.jbiotec.2013.11.005

Endo et al., 2007; Jez et al., 1997; Peralba et al., 1999; Ruiz et al., 2012). These AKRs have been reported not only to oxidize retinol and but also to reduce retinal. However, bacterial AKRs for retinal have not yet been characterized.

In this study, the *AKR* gene from *Marivirga tractuosa* was cloned and expressed in *Escherichia coli* for retinal reduction. The reaction conditions of the enzyme, including organic solvent, anti-oxidant, pH, temperature, and the concentrations of substrate and enzyme, were optimized. Under the optimized conditions, the production of all-*trans*-retinol from all-*trans*-retinal was performed. Moreover, the elucidation on the activity of *M. tractuosa* AKR for all-*trans*-retinol was tried.

2. Materials and methods

2.1. Bacterial strains, plasmid, and culture conditions

The expression vectors pET-22b(+) and pET-15b(+) were purchased from Novagen (San Diego, CA, USA). The expression host, *E. coli* ER 2566, and all restriction enzymes were purchased from New England Biolabs (Hertfordshire, UK). Luria-Bertani (LB) medium was purchased from BD Biosciences (San Jose, CA, USA). The substrates retinal and retinol and the cofactors NADH, NADPH, NAD^+, and $NADP^+$ (purity > 99%) were purchased from USB (Santa Clara, CA, USA). Pre-stained protein makers for SDS-PAGE and gel filtration calibration kit were purchased from MBI Fermentas (Hanover, MD, USA) and GE Healthcare (Piscataway, NJ, USA), respectively.

2.2. Gene cloning and site-directed mutagenesis

The gene encoding a putative AKR was amplified by PCR using the genomic DNA of *M. tractuosa* KCTC 2958 as a template. Sequences of primers used for gene cloning were based on DNA sequence of AKR from *M. tractuosa* DSM4126 (GenBank accession number NC_017459). Forward (5′-GCGGGATCCGATGAGAAAATT AACTTTCAGAAAC-3′) and reverse (5′-ATACTCGAGAGTTTCTCCCAAAGGCCAGCCATG-3′) primers for the insertion of pET-22b(+) plasmid were designed to introduce the underlined *Bam*HI and *Xho*I restriction sites, respectively, and forward (5′-GGCCATATGAGAAAATTAACTTTCAGAAAC-3′) and reverse (5′-ATACTCGAGTTCTCCCAAAGGCCAGCCATG-3′) primers for the insertion of pET-15b(+) plasmid were designed to introduce the underlined *Nde*I and *Xho*I restriction sites, respectively. The primers were synthesized by Bioneer (Daejon, Korea). The amplified DNA fragment was purified using a PCR purification kit (Promega, Fitchburg, WI, USA) and ligated into the *Bam*HI and *Xho*I sites of pET-22b(+) and the *Nde*I and *Xho*I sites of pET-15b(+). Each plasmid was transformed into *E. coli* ER2566 as an expression host, the transformed host was grown on LB agar (1.0% tryptone, 0.5% yeast extract, 1.0% sodium chloride, and 1.5% agar), and an ampicillin-resistant colony was selected. Gene expression was evaluated by both sodium dodecyl sulphate-polyacrylamide gel electrophoresis (SDS-PAGE) and enzyme activity assay. Mutations of the NADPH-binding residues in *M. tractuosa* AKR were generated by site-directed mutagenesis using a QuickChange Kit (Stratagene, Beverly, MA). DNA sequencing was performed at the Macrogen facility (Seoul, Korea).

2.3. Culture conditions and enzyme expression

M. tractuosa was grown in 50 ml of growth medium containing 0.5% glucose, 0.5% yeast extract, 1.0% casein peptone, and 0.5% sodium chloride in a 250 ml flask at 37 °C with shaking at 200 rpm. For protein expression, the recombinant *E. coli* cells were grown in LB medium in a 2000 ml flask containing 20 μg ml^{-1} ampicillin at 37 °C with shaking at 200 rpm. At the culture optical density of 0.6 at 600 nm, isopropyl-β-D-thiogalactopyranoside (IPTG) was added at a final concentration of 0.1 mM. For the enzyme expression, the culture was then incubated for additional 16 h at 16 °C with shaking at 150 rpm. The expression of *M. tractuosa* AKR was determined by SDS-PAGE.

2.4. Enzyme purification

The cells were harvested from the culture broth by centrifugation at 6000 × *g* for 30 min at 4 °C, washed twice with 0.85% NaCl, resuspended in 50 mM phosphate buffer (pH 8.0) containing 300 mM KCl and 10 mM imidazole, and disrupted on ice using a sonicator. The unbroken cells and cell debris were removed by centrifugation at 13,000 × *g* for 20 min at 4 °C and the supernatant was filtered through a 0.45-μm filter. The recombinant protein, which was expressed from pET-22b(+), was applied to an immobilized metal ion affinity chromatography cartridge (Bio-Rad, Hercules, CA, USA) equilibrated with 50 mM phosphate buffer (pH 8.0). The cartridge was washed extensively with the same buffer, and the bound protein was eluted with a linear gradient of 10–500 mM imidazole at a flow rate of 1 ml min^{-1}. The eluate was collected and loaded onto a Bio-Gel P-6 desalting cartridge (Bio-Rad) equilibrated with 50 mM *N*-(2-hyroxyethyl)piperazine-*N*′-(3-propanesulfonic acid) (HEPPS) buffer (pH 7.5). The protein was eluted with 50 mM HEPPS buffer (pH 7.5) at a flow rate of 1 ml min^{-1} to obtain a solution of purified enzyme. The hexahistidine tag of the recombinant protein, which was expressed from pET-15b(+), was cut with a thrombin capture kit (Novagen, Madison, WI, USA). The thrombin-treated enzyme was applied to a His-trap HP affinity chromatography column (GE Healthcare, Piscataway, NJ, USA) equilibrated with 50 mM phosphate buffer (pH 7.0) for removing the histidine tag. The active factions were pooled and subsequently loaded onto a Benzamidine Sepharose column (Novagen, Madison, WI, USA) equilibrated with 50 mM phosphate buffer (pH 8.0) for removing thrombin. The columns were eluted in 50 mM HEPPS buffer (pH 7.5) at a flow rate of 1 ml min^{-1}. The resulting solution was used as a purified untagged protein, which was confirmed by SDS-PAGE. All purification steps using cartridges were carried out in a cold room at 4 °C with a Profinia protein purification system (Bio-Rad).

2.5. Determination of molecular mass

The subunit molecular mass of AKR from *M. tractuosa* was examined by SDS-PAGE (12% gels) under denaturing conditions, using the prestained protein makers as reference proteins. All protein bands were stained with Coomassie blue for visualization. The molecular mass of the native enzyme from *M. tractuosa* was determined by gel filtration chromatography using Sephacryl S-300 preparative-grade column HR 16/60 (GE Healthcare). The purified enzyme solution was applied to the gel filtration column and eluted at a flow rate of 0.3 ml min^{-1} with 50 mM HEPPS buffer (pH 7.5) containing 150 mM NaCl. The column was calibrated with ferritin (453 kDa), catalase (206 kDa), ovalbumin (44 kDa), and carbonic anhydrase (29 kDa) as reference proteins (GE Healthcare). The molecular mass of the native AKR was calculated by comparing with the migration time of the enzyme to those of the reference proteins.

2.6. Enzyme assay

Unless otherwise stated, the reaction was performed at 30 °C in 50 mM HEPPS buffer (pH 7.5) containing 0.2 mM all-*trans*-retinal, 0.016 unit ml^{-1} (0.05 mg ml^{-1}) enzyme, 5% (v/v) methanol, 1% (w/v) hydroquinone, and 1 mM NADPH for 5 min. After incubation, the reaction was stopped by adding the same volume of absolute

methanol to the reaction solution. The mixture was extracted with the same volume of *n*-hexane, and additional vortexing was performed for 1 min. After centrifugation at 13,000 × *g* for 10 min at 4 °C, the supernatant was used for analysis. The concentrations of all-*trans*-retinal as a substrate and all-*trans*-retinol as a reaction product were determined by HPLC system as described below. One unit of AKR activity was defined as the amount of enzyme required to produce 1 μmol of all-*trans*-retinol per min from all-*trans*-retinal at 30 °C and pH 7.5.

2.7. Effects of pH and temperature on enzyme activity

To examine the effect of pH on enzyme activity, the pH values were varied from 6.5 to 8.5 using 50 mM piperazin-*N*,*N*′-ethanesulfonic acid (PIPES) buffer (pH 6.5–7.5) and 50 mM HEPPS buffer (pH 7.5–8.5). The effect of temperature on enzyme activity was investigated by varying the temperature from 20 to 40 °C. The effect of temperature on enzyme stability was evaluated over the same temperature range for 120 min. Samples were withdrawn at specific time intervals and the residual relative activity was measured.

2.8. Effects of detergents, solvents, and antioxidants on enzyme activity

The effect of detergent on enzyme activity was investigated using Span 20, Span 80, Tween 20, Tween 40, Tween 80, and Triton X-100 at 0.05% (w/v). Solvents, including ethanol, methanol, acetone, formic acid, butanol, dimethyl sulfoxide, 1,4-dioxane, and propyl alcohol, were added to the reaction solution at the concentration of 1% (v/v). The effect of methanol concentration on enzyme activity was evaluated by varying its concentration from 0 to 15% (v/v). Antioxidants, butylated hydroxytoluene (BHT), butylated hydroxyanisole (BHA), tris(2-chloroethyl phosphate (TCEP), dithiothreitol (DTT), and hydroquinone were added to the reaction solution at the concentration of 1% (w/v) to find the optimum antioxidant. The effects of the concentrations of BHT and hydroquinone on the AKR activity were investigated by varying its concentration from 0 to 3% (w/v).

2.9. Cofactor and substrate specificity

NAD^+ and $NADP^+$ were used for the oxidation of alcohol substrates, while NADH and NADPH were used for the reduction of aldehyde substrates. The activity of *M. tractuosa* AKR was determined at 30 °C in 50 mM HEPPS buffer (pH 7.5) containing cofactor (0.1–5 mM), 0.2 mM all-*trans*-retinal, and 5% (v/v) methanol for 5 min. The aldehydes all-*trans*-retinal, 9-*cis*-retinal, 13-*cis*-retinal, acetaldehyde, and benzaldehyde, the alcohols all-*trans*-retinol, methanol and ethanol, the carbonyls acetone and oxaloacetate, and the monosaccharides glucose and fructose were used as substrates. The reactions were performed at 30 °C in 50 mM HEPPS buffer (pH 7.5) containing substrate, 5% (v/v) methanol, and 1 mM NADPH or $NADP^+$ for 5 min. The various concentrations of substrates (0.01–5 mM) were used to determine the kinetic parameters and 0.2 mM substrate was used to measure the activity of *M. tractuosa* AKR.

2.10. Production of all-trans-retinol from all-trans-retinal

The effect of substrate concentration on the conversion of all-*trans*-retinal by *M. tractuosa* AKR was investigated. The reactions were performed in 50 mM HEPPS buffer (pH 7.5) containing various amounts of all-*trans*-retinal (57–4270 mg l^{-1} or 0.2–15 mM), 0.016 unit ml^{-1} enzyme, 5% (v/v) methanol, 1% (w/v) hydroquinone, and 10 mM NADPH at 30 °C for 5 min. The effect of the enzyme concentration was evaluated with 1710 mg l^{-1} (6 mM) all-*trans*-retinal in the range of 0.016–4.5 unit ml^{-1} enzyme. The time course reactions were performed with 1710 mg l^{-1} all-*trans*-retinal and 3 unit ml^{-1} enzyme for 160 min.

2.11. Circular dichroism

Circular dichroism (CD) spectra of the wild-type and variant enzymes were recorded with a spectrophotometer (Jasco J-815, Tokyo, Japan) using a 0.5-cm path length quartz cell. Acquisition of far-UV (190–250 nm) CD spectra was performed in 50 mM HEPPS buffer (pH 7.5) containing 3 mg ml^{-1} enzyme at 20 °C with a rate of 100 nm min^{-1}. CD spectra were corrected for base line, and ellipticity for each sample was expressed in millidegrees.

2.12. Homology modeling and substrate docking calculation of binding energy

Homology modeling of *M. tractuosa* AKR was performed using Build Homology Models module in the MODELER application of Discovery Studio 3.1 (Accelrys Software, San Diego, CA, USA) based on the crystal structure of human AKR (AKR1B10) (Protein data bank, PDB, entry 1ZUA) as a template. Comparative modeling was used to generate the most probable structure of the query protein by aligning it with the template sequence, simultaneously considering spatial restraints, and local molecular geometry. The generated structure was improved by subsequent refinement of the loop conformations by assessing the compatibility of amino acid sequences with known PDB structures (Protein Health module, DS 3.1). The geometry of loop region was corrected using the Refine Loop/MODELER, and the best model was chosen. To confirm consistency of the model, the quality of the model was analyzed by PROCHECK software as a different validation tool (Laskowski et al., 1993). Hydrogen atoms were added to the model; these atoms were minimized to have stable energy conformation and to relax the conformation from close contacts. A sphere with a radius of 12 Å around the ligand-binding pocket of AKR defined its active site with Asp43, Tyr48, Lys77, and His110 residues. $NADP^+$ and NADPH were docked into the active-site pocket of the model of *M. tractuosa* AKR by using C-DOCKER module. Candidate poses were created using random rigid-body rotations, followed by simulated annealing. The structures of the protein, cofactor, and their complexes were subjected to energy minimization using the CHARMM force field in DS 3.1 (Al-Balas et al., 2012). Full-potential final minimization was used to refine the substrate poses. The energy-docked conformation of the substrate was retrieved for postdocking analysis using C-DOCKER module. The substrate orientation giving the lowest interaction energy was chosen for subsequent rounds of docking. To estimate the binding energy between a receptor and a ligand, the binding energy was calculated using the equation $\mathrm{Energy_{Binding}} = \mathrm{Energy_{complex}} - \mathrm{Energy_{Ligand}} - \mathrm{Energy_{Receptor}}$ (Tirado-Rives and Jorgensen, 2006).

2.13. Analytical methods

The same volume of acetonitrile was added to the reaction solution, and the resulting solution was mixed and kept on ice for 5 min. After centrifugation at 10,000 × *g* for 30 min at 4 °C, substrate and product in the supernatant were analyzed by an HPLC system (Agilent 1200 series, Santa Clara, CA, USA) equipped with a UV detector at 350 nm and an Atlantis dC18 column (Waters, Milford, MA, USA). The product was eluted with a mixture of acetonitrile and 1% ammonium acetate in water with 80:20 (v/v) as the mobile phase with a flow rate of 1.2 ml min^{-1} at 30 °C. The substrates all-*trans*-retinal, 9-*cis*-retinal, and 13-*cis*-retinal were detected with retention times of 11.3, 18.8, and 18.6 min,

respectively. The products all-*trans*-retinol, 9-*cis*-retinol, and 13-*cis*-retinol were detected with retention times of 8.0, 13.5, and 12.4 min, respectively. The concentrations of glucose and fructose were determined using a Bio-LC system (Dionex ICS-3000, Sunnylvale, CA) with an electrochemical detector and a CarboPac PA1 column. The column was eluted at 30 °C with 200 mM sodium hydroxide at a flow rate of 1 ml min^{-1}. The activity of the enzyme for acetaldehyde and benzaldehyde were assayed at 30 °C by mearsuring decrease in NADPH absorbance at 340 nm (Yim et al., 2004).

3. Results

3.1. Gene cloning and molecular mass of AKR from M. tractuosa

The *Ftrac_3685* gene (951 bp) previously proposed as the putative AKR gene of *M. tractuosa* (GenBank accession number NC_014759.1) was cloned and expressed in *E. coli*. The expressed enzyme was purified by immobilized metal ion affinity chromatography. The purified protein showed a single band in SDS-PAGE with a molecular mass of approximately 37 kDa (Fig. 1a), which is consistent with the calculated value of 36.8 kDa based on the 316-residue sequence plus the hexa-histidine tag as determined with the Compute pI/Mw tool on the ExPASy server. The native protein from *M. tractuosa* AKR was determined by gel filtration chromatography to be 72 kDa, indicating that it is a dimer (Fig. 1b). However, mammalian AKRs were identified as monomers (35–37 kDa) (Cao et al., 1998; Gallego et al., 2006; Jia et al., 2006).

3.2. Effects of detergents, solvents, and antioxidants on the activity of M. tractuosa AKR

The activity of *M. tractuosa* AKR decreased with the addition of any detergent (data not shown). The enzyme activity for all-*trans*-retinal was the highest using methanol among the solvents tested (Fig. 2a), and its optimal concentration was 5% (v/v) (Fig. 2b). The enzyme activity in water for all-*trans*-retinal was very low because the substrate was nearly insoluble in water. The addition of antioxidants, including BHT, BHA, TCEP, DTT, and hydroquinone, increased the enzyme activity. The reaction samples in the presence of antioxidants with an increasing stability of retinal showed the higher contents of retinal than those in the absence of antioxidants. When BHT or hydroquinone was added, the activity for all-*trans*-retinal reduction was higher than those of the other antioxidants (Fig. 3a). The optimal concentration of these antioxidants was 1% (w/v), and the activity of *M. tractuosa* AKR at the concentration increased approximately 1.4-fold (Fig. 3b). Therefore, the hydrophilic hydroquinone (Akhavan and Levitt, 2008) at 1% was added before the enzyme reaction and the hydrophobic BHT (Tsunoda and Takabayashi, 1995) at 1% was added after the reaction in all subsequent experiments.

3.3. Effects of pH and temperature on the activity of M. tractuosa AKR

The enzymatic conversion of all-*trans*-retinal into all-*trans*-retinol was examined in pH range of 6.5–8.5 in the presence of 5% (v/v) methanol and 1% (w/v) hydroquinone (Fig. 4a). The maximum activity was observed at pH 7.5. The effect of temperature on the enzyme activity was shown in Fig. 4b, and the maximum activity was observed at 30 °C. To investigate the effect of temperature on enzyme stability, the enzyme was incubated at a temperautre ranging from 0 to 70 °C for 120 min. The enzyme activity decreased slightly after incubation at temperatures below 30 °C, but dropped significantly at temperatures above 30 °C. The enzyme activity at 60 °C was 24% of that at 0 °C (Fig. 4c).

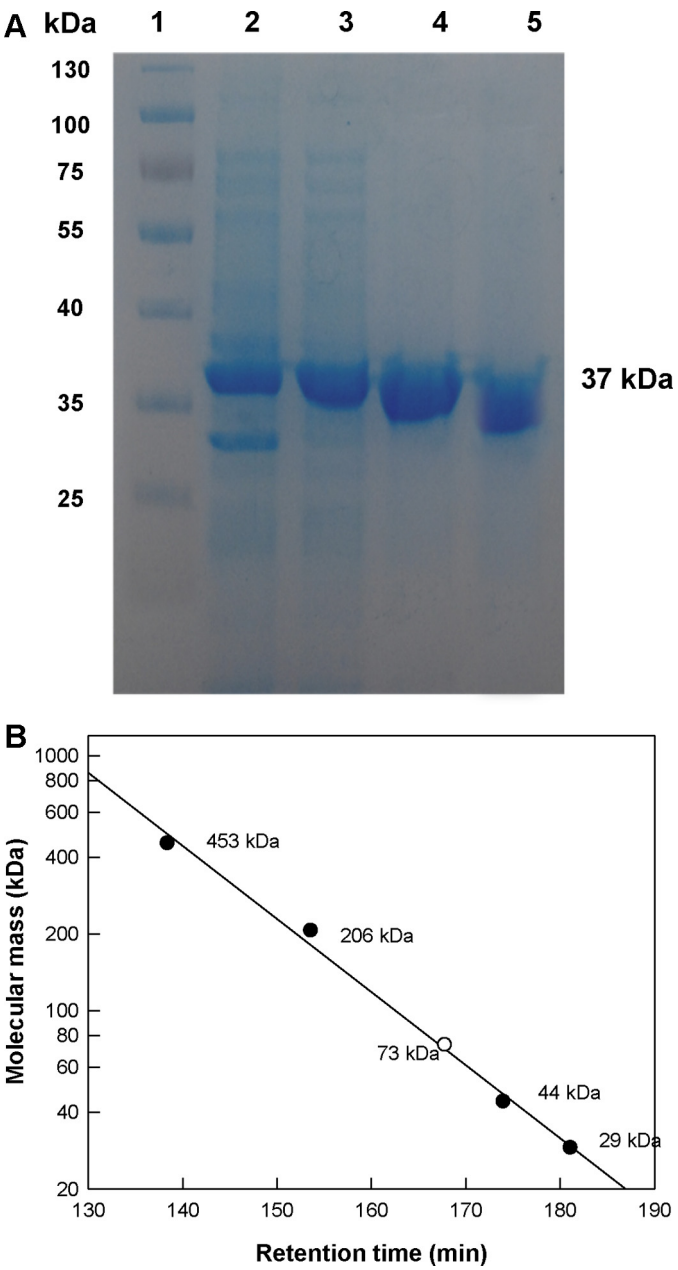

Fig. 1. (A) SDS-PAGE stained with Coomassie blue of the purified AKR from *M. tractuosa*. Lane 1, molecular mass protein markers; lane 2, inclusion bodies; lane 3, crude extract; lane 4, purified hexa-histidine tagged AKR; lane 5, purified untagged AKR. (B) Determination of molecular mass of the purified native enzyme using Sephacryl S-300 HR gel filtration chromatography. The reference proteins were ferritin (453 kDa), catalase (206 kDa), ovalbumin (44 kDa), and carbonic anhydrase (29 kDa). The enzyme was eluted at a retention time corresponding to 70 kDa.

3.4. Cofactor and substrate specificity

The cofactor specificity of *M. tractuosa* AKR was investigated using all-*trans*-retinal. The enzyme was inactive for NAD^+, $NADP^+$, or NADH as a cofactor but active for NADPH. The concentration of NADPH was used at 1 mM for 0.2 mM all-*trans*-retinal. The specific activity of *M. tractuosa* AKR in the presence of NADPH followed the order benzaldehyde > acetaldehyde > all-*trans*-retinal > 9-*cis*-retinal. No activity was observed for 13-*cis*-retinal (Table 1). The order for k_{cat} was the same as that for specific activity. However, the K_m for all-*trans*-retinal was 32- and 40-fold lower than those

Table 1
Kinetic parameters of *M. tractuosa* AKR for aldehyde substrates, and binding energy after substrate docking.

Substrate	Specific activity (nmol mg^{-1} min^{-1})	K_m (μM)	k_{cat} (min^{-1})	k_{cat}/K_m (mM^{-1} min^{-1})	ΔE_{bind} (kcal mol^{-1})
All-*trans*-retinal	319 ± 5.4	48 ± 4.2	21.5 ± 0.5	427 ± 1.6	−46.85
9-*cis*-retinal	43 ± 0.5	225 ± 9.1	1.6 ± 0.0	8 ± 0.6	−21.72
13-*cis*-retinal	ND				
Acetaldehyde	1444 ± 21	1919 ± 3	101 ± 1.5	52 ± 0.9	−2.16
Benzaldehyde	5911 ± 81	1516 ± 26	446 ± 3.6	294 ± 1.4	−17.71

ND, specific activity is not detected by the analytical methods used in this study.
Data represent means of three experiments and ± represents standard deviations.

for benzaldehyde and acetaldehyde, respectively. As a result, the catalytic efficiency (k_{cat}/K_m) of *M. tractuosa* AKR for all-*trans*-retinal was the highest among the tested substrates (427 mM^{-1} min^{-1}), which was 1.5- and 8.2-fold higher than those for benzaldehyde (294 mM^{-1} min^{-1}) and acetaldehyde (52 mM^{-1} min^{-1}), respectively.

3.5. Production of all-trans-retinol from all-trans-retinal by M. tractuosa AKR

The enzymatic production of all-*trans*-retinol from all-*trans*-retinal was examined with 0.016 unit ml^{-1} enzyme in the presence of 5% (v/v) methanol, 1% (w/v) hydroquinone, and 10 mM NADPH

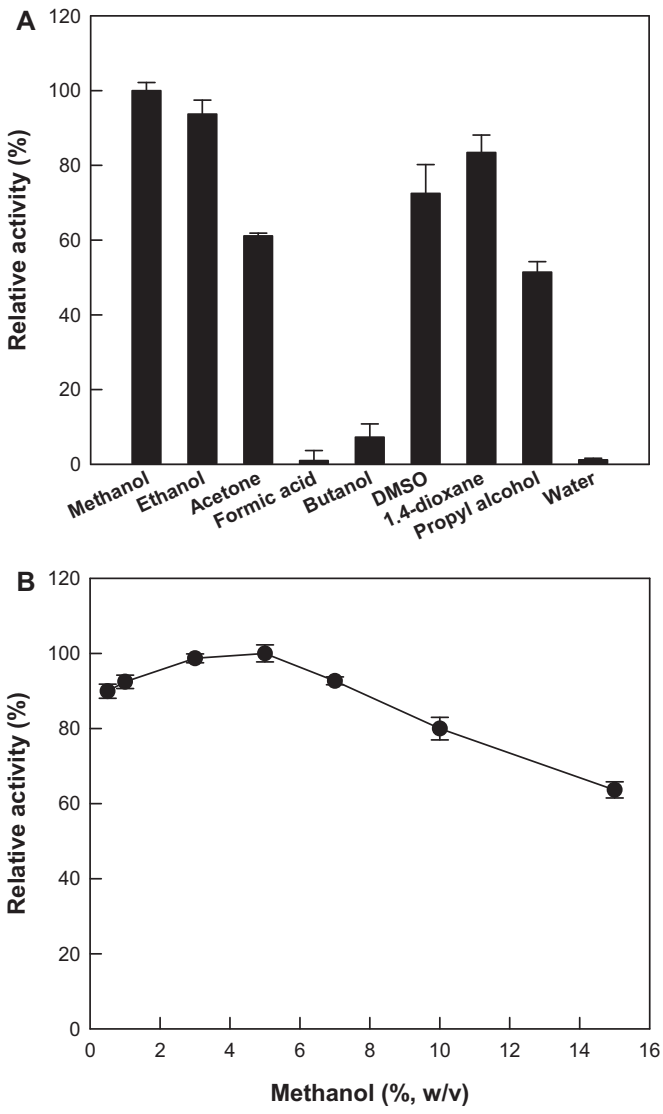

Fig. 2. Effect of organic solvent on the activity of *M. tractuosa* AKR. (A) Effect of solvent kind. The reactions were performed at 30 °C in 50 mM PIPES buffer (pH 7.5) containing 0.2 mM all-*trans*-retinal, 0.016 unit ml^{-1} enzyme, 1% (v/v) solvent, and 1 mM NADPH for 5 min. (B) Effect of methanol concentration. The reactions by varying concentration of methanol were performed at 30 °C in 50 mM PIPES buffer (pH 7.5) containing 0.2 mM all-*trans*-retinal, 0.016 unit ml^{-1} enzyme, and 1 mM NADPH for 5 min. Data represent the means of three experiments and error bars represent standard deviation.

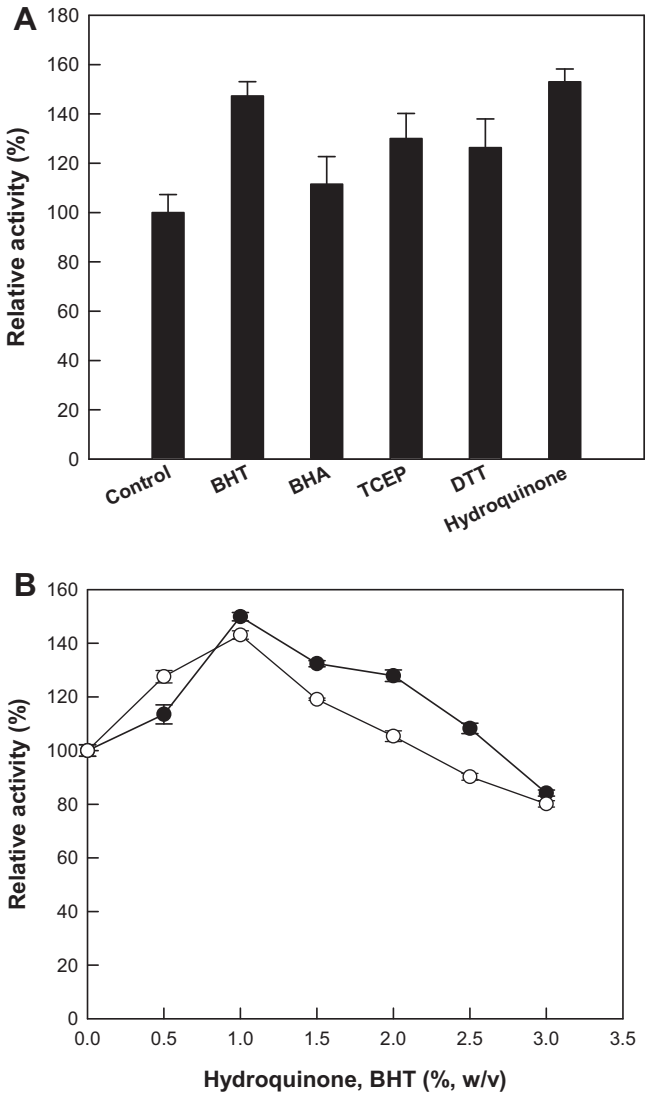

Fig. 3. Effect of anti-oxidant on the activity of *M. tractuosa* AKR. (A) Effect of anti-oxidant kind. The reactions were performed at 30 °C in 50 mM PIPES buffer (pH 7.5) containing 0.2 mM all-*trans*-retinal, 0.016 unit ml^{-1} enzyme, 5% (v/v) methanol, 1% (v/v) anti-oxidant, and 1 mM NADPH for 5 min. (B) Effect of anti-oxidant concentration. The reactions by varying concentration of hydroquinone or BHT were performed at 30 °C in 50 mM PIPES buffer (pH 7.5) containing 0.2 mM all-*trans*-retinal, 0.016 unit ml^{-1} enzyme, 5% (v/v) methanol, and 1 mM NADPH for 5 min. Data represent the means of three experiments and error bars represent standard deviation.

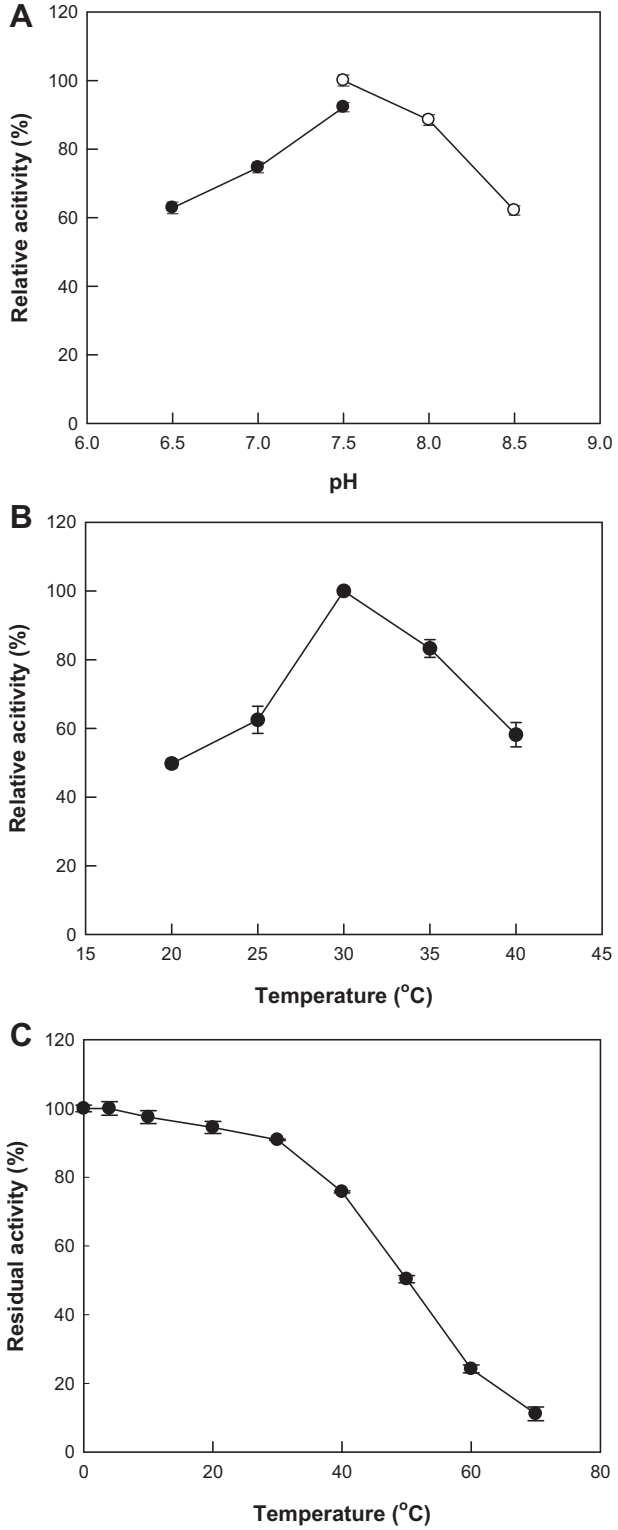

Fig. 4. Effects of pH and temperature on the activity of *M. tractuosa* AKR. (A) Effect of pH on enzyme activity. The reactions were performed in 50 mM PIPES buffer for pH 6.5 to 7.5 (•) and 50 mM HEPPS buffer for pH 7.5 to 8.5 (○) with 0.2 mM all-*trans*-retinal, 0.016 unit ml^{-1} enzyme, 5% (v/v) methanol, 1% (v/v) hydroquinone, and 1 mM NADPH at 30 °C for 5 min. (B) Effect of temperature on enzyme activity. The reactions were performed in 50 mM PIPES buffer (pH 7.5) containing 0.2 mM all-*trans*-retinal, 0.016 unit ml^{-1} enzyme, 5% (v/v) methanol, 1% (v/v) hydroquinone, and 1 mM NADPH for 5 min in temperature range of from 15 to 35 °C. (C) Effect of temperature on enzyme stability. The enzyme was incubated at temperatures from 0 to 70 °C for 120 min. The residual relative activity was measured in 50 mM HEPPS buffer (pH 7.5) containing 0.2 mM retinal, 0.016 unit ml^{-1} enzyme, 5% (v/v) methanol, 1% (v/v) hydroquinone, and 1 mM NADPH at 30 °C for 5 min. Data represent the means of three experiments and error bars represent standard deviation.

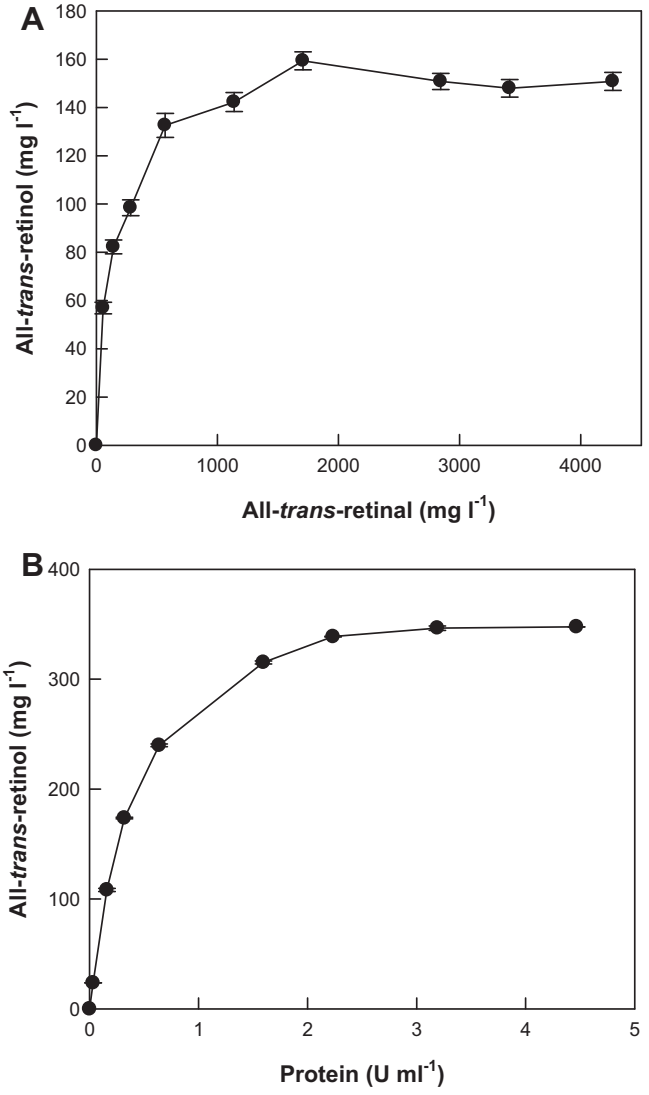

Fig. 5. Effects of the concentrations of substrate and enzyme on all-*trans*-retinol production from all-*trans*-retinal by *M. tractuosa* AKR. (A) Effect of substrate concentration. The reactions were performed as a substrate in 50 mM HEPPS buffer (pH 7.5) containing 0.016 unit ml^{-1} enzyme, 5% (v/v) methanol, 1% (v/v) hydroquinone, and 10 mM NADPH at 30 °C for 5 min. (B) Effect of enzyme concentration. The reactions were performed in 50 mM HEPPS buffer (pH 7.5) containing 6 mM all-*trans*-retinal, 3 unit ml^{-1} enzyme, 5% (v/v) methanol, 1% (v/v) hydroquinone, and 10 mM NADPH at 30 °C for 5 min.

as a sufficient amount by varying the substrate concentration from 57 (0.2) to 4270 mg l^{-1} (15 mM). Up to 1710 mg l^{-1} (6 mM) all-*trans*-retinal, all-*trans*-retinol production increased with increasing the all-*trans*-retinal concentration, however, above 1710 mg l^{-1} all-*trans*-retinal, it reached a plateau (Fig. 5A). Thus, the optimal all-*trans*-retinal concentration was determined to be 1710 mg l^{-1}. All-*trans*-retinol production was investigated at the enzyme concentration ranging from 0.032 to 4.47 unit ml^{-1} enzyme with 1710 mg l^{-1} all-*trans*-retinal as the substrate after 5 min (Fig. 5B) All-*trans*-retinol production increased with increasing the enzyme concentration up to 3 unit ml^{-1} and reached a plateau at the concentration above 3 unit ml^{-1}. Thus, the optimal enzyme concentration was determined to be 3 unit ml^{-1}.

The optimal reaction conditions for the production of all-*trans*-retinol from all-*trans*-retinal by *M. tractuosa* AKR were pH 7.5, 30 °C, 5% (v/v) methanol, 1% (w/v) hydroquinone, 10 mM NADPH, 1710 mg l^{-1} all-*trans*-retinal, and 3 unit ml^{-1} enzyme. Under these optimized conditions, time-course reactions of

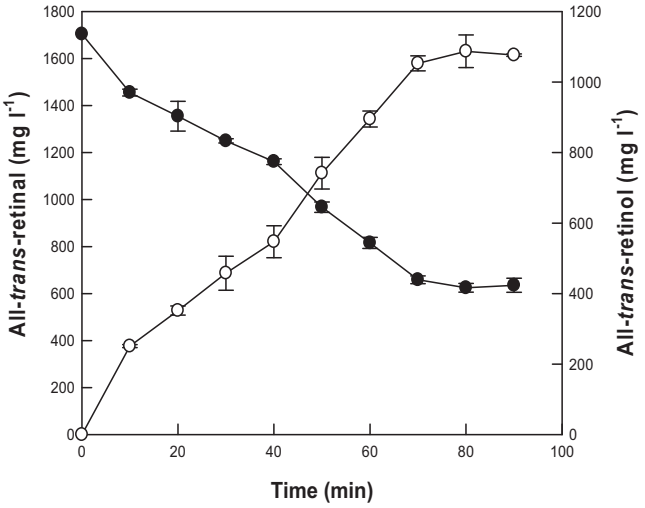

Fig. 6. Time course reactions of all-*trans*-retinol production from all-*trans*-retinal by *M. tractuosa* AKR. The reactions of all-*trans*-retinol (○) production from all-*trans*-retinal (●) were performed by varying the reaction time in 50 mM HEPPS buffer (pH 7.5) containing 1710 mg l^{-1} all-*trans*-retinal, 3 unit ml^{-1} enzyme, 5% (v/v) methanol, 1% (v/v) hydroquinone, and 10 mM NADPH at 30 °C for 160 min. Data represent the means of three experiments and error bars represent standard deviation.

all-*trans*-retinol production from all-*trans*-retinal were performed for 90 min (Fig. 6). The enzyme reduced all-*trans*-retinal at its aldehyde group to yield all-*trans*-retinol in a 1:1 molar ratio during the reaction. After 80 min, the concentration of all-*trans*-retinol was approximately 1090 mg l^{-1} (3.8 mM),with a conversion yield of 64% (w/w) and a volumetric productivity of 818 mg l^{-1} h^{-1}. However, under the same conditions, the enzymatic reaction for all-*trans*-retinol as a substrate did not occur and then all-*trans*-retinal as a product was not detected by the analytical methods used in this study.

4. Discussion

The activity of AKR for aldehyde and retinal substrates has been reported in many mammals (Crosas et al., 2001; Duester, 2000; Jez et al., 1997; Peralba et al., 1999; Ruiz et al., 2012). *M. tractuosa* AKR has activity for the aldehyde substrates benzaldehyde, acetaldehyde, all-*trans*-retinal, and 9-*cis*-retinal. However, the enzyme did not have activity for the alcohol substrates all-*trans*-retinol, ethanol, and methanol, the carbonyl substrates acetone and oxaloacetate, and the monosaccharide substrates glucose and fructose. These results indicate that *M. tractuosa* AKR is an aldehyde reductase.

The recombinant *M. tractuosa* AKR expressed from pET-22b(+) had a hexa-histidine tag at the carboxyl terminus. To investigate the effect of histidine tag on the kinetic parameters of the enzyme, the histidine tag in the recombinant *M. tractuosa* AKR, which was expressed from pET-15b, was removed by treating thrombin. The k_{cat} (23.8 min^{-1}) and K_m (44 μM) of *M. tractuosa* AKR without histidine tag for all-*trans*-retinal were 11% higher and 9% lower than those of *M. tractuosa* AKR with histidine tag, respectively. Thus, histidine tag of *M. tractuosa* AKR resulted in a little decrease in the turnover rate and affinity. AKR is well known as a retinal reducing enzyme with a higher k_{cat}/K_m compared to any other AKR family enzymes (Endo et al., 2009). However, there are no data on bacterial AKRs that convert retinal. Therefore, in this study, AKR from *M. tractuosa* was characterized as a representative of a bacterial AKR.

The amino acid sequence of AKR from *M. tractuosa* has 43, 42, 43, and 42% identity with the human AKR1A1 (Alzeer and Ellis, 2011), AKR1B1 (Cao et al., 1998), and AKR1B10 (Gallego et al., 2006), and the mouse AKR1A4 (Jia et al., 2006), respectively, and exhibited 21, 31, and 16% identity with *Bacillus subtilis* AKR11A (Yoshida et al., 1995), *Corynebacterium* sp. AKR5C (Miller et al., 1987), and *E. coli* AKR14A1 (Grant et al., 2003), respectively. The catalytic residues are absolutely conserved not only in the bacterial AKRs but also in the mammalian AKRs. However, cofactor-binding residues showed certain differences (Fig. 7).

The homology models based on the sequence identity between 30 and 60% to template structure can be used for protein engineering and supporting site-directed mutagenesis studies and may be used for substrate docking (Marti-Renom et al., 2000). AKR from *M. tractuosa* has 42% identity with the identified crystal structure of the human AKR1B10 (PDB entry 1ZUA). Thus, the docking of substrate and cofactor using the homology model based on the human AKR1B10 could be performed to find cofactor-binding residues of *M. tractuosa* AKR. However, the actual structure of *M. tractuosa* AKR complexed with substrate must be obtained to provide exact evidence. The homology model of *M. tractuosa* AKR shows a classical α/β TIM barrel structure commonly found in the AKR family (Mindnich and Penning, 2009), which consists of the cofactor-binding (residues 19–21, 158–159, 206–213, 259–271) and catalytic (Tyr 48) domains. In the model, the active site residues exhibited locations and orientations similar to the template, human AKR (AKR1B10) (data not shown). In the model after docking of $NADP^+$ and all-*trans*-retinal, Asp43, Tyr48, Lys77, His110, Ala 158, Lys 212, and Gln170 were identified as cofactor-binding residues of *M. tractuosa* AKR.

Mammal AKRs catalyze the reversible reactions, converting all-*trans*-retinal to all-*trans*-retinol and *vice versa* (Endo et al., 2009; Fukumoto et al., 2005; Martin et al., 2006). However, *M. tractuosa* AKR exhibited no activity for all-*trans*-retinol with $NADP^+$ as a cofactor. Cofactor-binding residues are involved in the reactions of oxidation and reduction. Superimposition of the cofactor-binding domains of human and *M. tractuosa* AKRs shows that the key cofactor-binding residues in human AKR, Ser160, Pro216, and Glu272 (Fig. 8a) are different with those of *M. tractuosa* AKR such as Ala 158, Lys 212, and Gln 270, respectively (Fig. 8b). To determine the role of these residues, site-directed mutagenesis was performed (Table 2). Lys212, Ala158, and Gln270 in *M. tractuosa* AKR were replaced with proline, serine, and glutamic acid (aspartic acid) in human AKR1B10, respectively, to identify the differences between human and *M. tractuosa* AKRs. Moreover, the positive charged residue Lys212 was replaced with the non-bulky residue alanine, the negative charged residue glutamic acid, or the positive charged residue arginine with a different length, respectively; Ala158 was substituted with asparagines or tyrosine that could form hydrogen bonds to cofactor like serine, respectively; and the negative charged residue Gln270 was replaced with the non-bulky residue alanine or the positive charged residue arginine, respectively. Substitution of Lys212 with alanine, glutamic acid, proline, or arginine resulted in no change on the activity for all-*trans*-retinol, indicating that Lys212 is not a critical cofactor-binding residue. The A158N and Q270R variants had no activity for all-*trans*-retinal and all-*trans*-retinol, whereas the A158S, Q270D, and Q270E variants showed activity. The activity of the Q270D variant for all-*trans*-retinol was too low. The K_m, k_{cat}, and k_{cat}/K_m values of the A158S variant for all-*trans*-retinol were 55 μM, 0.74 min^{-1}, 13 mM^{-1} min^{-1} respectively, and those of the Q270E variant were 405 μM, 1.8 min^{-1}, 5 mM^{-1} min^{-1}, respectively.

Ser160 of human AKR, which corresponds to Ala158 of *M. tractuosa* AKR, is known to be $NADP^+$-binding residue in the reaction of alcohol oxidation (Jez et al., 1997; Ruiz et al., 2011). Ser160 and Glu272 of human AKR formed hydrogen bonds with $NADP^+$ (Fig. 8c and e), whereas Ala158 and Gln270 of *M. tractuosa* AKR did not (Fig. 8d and f). The conformational changes of the wild-type and

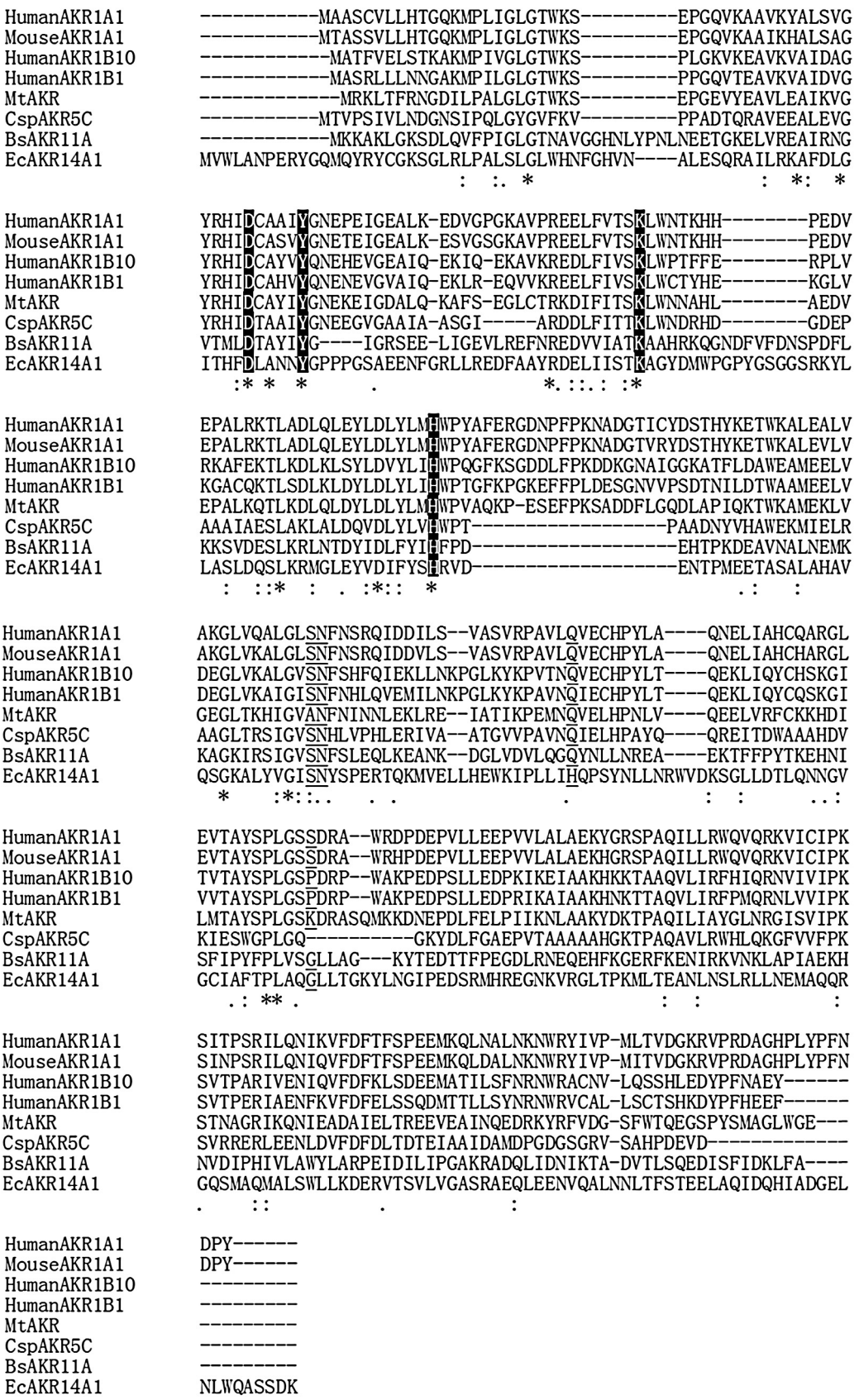

Fig. 7. Sequence alignment of *M. tractuosa* AKR, the human AKR1A1, AKR1B1, and AKR1B10, the mouse AKR1A1, *B. subtilis* AKR11A, *Corynebacterium* sp. AKR5C, and *E. coli* AKR14A1. The GenBank accession numbers of the human AKR1A1, AKR1B1, and AKR1B10, the mouse AKR1A1, *M. tractuosa* AKR, *B. subtilis* AKR11A, *Corynebacterium* sp. AKR5 C, and *E. coli* AKR14A1 are AAB92369.1, AAA51714.1, AAC36465.1, BAB27907.1, ADR23652.1, BAA21607.1, AAA83534.1, and AAG58137.1, respectively. The predicted catalytic residues of *M. tractuosa* AKR (Asp43, Tyr48, Lys77, and His110) are highlighted in white on black background. The cofactor-binding residues of *M. tractuosa* AKR (Ala158, Asn159, Gln180, Lys212, and Gln270) are underlined. Sequence alignment was performed using CLUSTAL W program. Asterisk, colon, and dot represent identity, conserved substitution, and semi-conserved substitution, respectively.

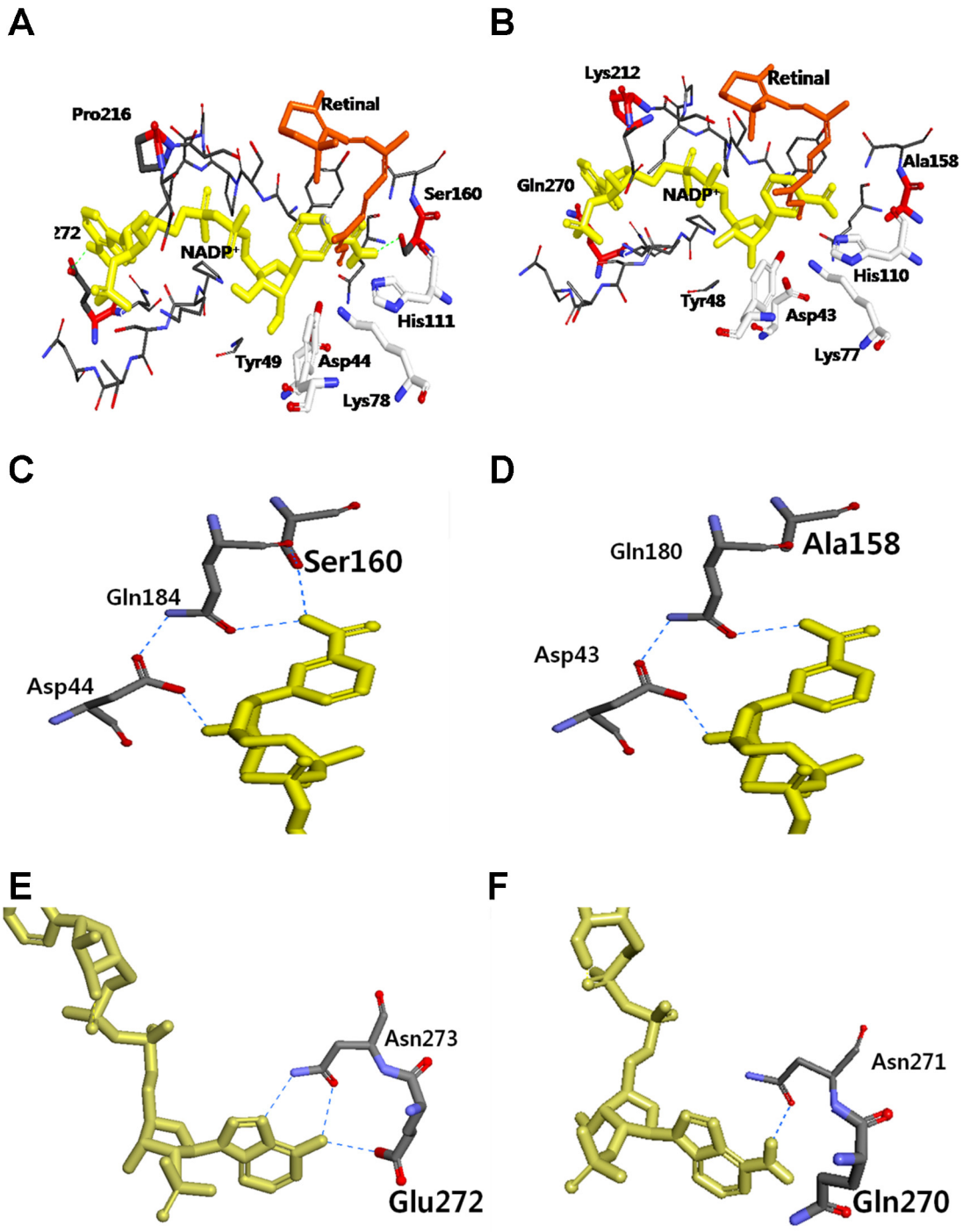

Fig. 8. Critical cofactor-binding residues of human and *M. tractuosa* AKRs. Docking of $NADP^+$ to human AKR or *M. tractuosa* AKR in the homology model. (A) Structure of the active site in human AKR with all-*trans*-retinal as a substrate and $NADP^+$ as a cofactor. (B) Structure of the active site in *M. tractuosa* AKR with all-*trans*-retinal as a substrate and $NADP^+$ as a cofactor. (C) Ser160 of human AKR. (D) Ala158 of *M. tractuosa* ARL. (E) Glu272 of human aldo-keto reductase. (F) Gln270 of *M. tractuosa* AKR. $NADP^+$, all-*trans*-retinal, oxygen, nitrogen, and carbon are colored with yellow, orange, red, blue, and gray, respectively. Line indicates a hydrogen bond.

variant enzymes were investigated using CD (McHarg et al., 1999; Tien Le et al., 2003). The CD spectra of the A158S and Q270E variants showed similar patterns compared to the wild-type enzyme (Supplementary Fig. 1), indicating that the mutations did not affect the AKR secondary structure. The increased hydrogen bonding to $NADP^+$ in the A158S or Q270E variant may show its capacity to oxidize all-*trans*-retinol (Kavanagh et al., 2003). Thus, no activity of *M. tractuosa* AKR for all-*trans*-retinol may be due to lack of the binding of Ala158 and Gln270 to $NADP^+$.

The turnover numbers (k_{cat}) followed the order benzaldehyde > acetaldehyde > all-*trans*-retinal > 9-*cis*-retinal (Table 1) and their chemical structures are shown in Supplementary Fig. 2. In the homology model, the distance between the catalytic residue (Tyr48) and the aldehyde group of benzaldehyde, acetaldehyde, all-*trans*-retinal, or 9-*cis*-retinal obtained from docking studies was 2.4, 2.9, 3.1, or 6.9 Å, respectively. The shorter distance between the catalytic residue (Tyr48) and a substrate may result in a higher turnover rate. *M. tractuosa* AKR showed the highest k_{cat}/K_m and the

Table 2
Kinetic parameters of the wild-type and variant enzymes in the cofactor-binding domain of *M. tractuosa* AKR.

Enzyme	Substrate	Specific activity (nmol mg^{-1} min^{-1})	K_m (μM)	k_{cat} (min^{-1})	k_{cat}/K_m (mM^{-1} min^{-1})
Wild-type	All-*trans*-retinal	319 ± 5.4	48 ± 4.2	21.5 ± 0.5	427 ± 4.4
	All-*trans*-retinol	NC			
A158N	All-*trans*-retinal	NC			
	All-*trans*-retinol	NC			
A158S	All-*trans*-retinal	438 ± 1.6	29 ± 2.3	20.9 ± 0.3	703 ± 1.1
	All-*trans*-retinol	21 ± 0.2	55 ± 1.3	0.74 ± 0.0	13 ± 0.3
A158Y	All-*trans*-retinal	0.3 ± 0.0			
	All-*trans*-retinol	NC			
K212A	All-*trans*-retinal	157 ± 0.3	68 ± 2.2	13.2 ± 0.0	189 ± 3.1
	All-*trans*-retinol	NC			
K212E	All-*trans*-retinal	NC			
	All-*trans*-retinol	NC			
K212P	All-*trans*-retinal	185 ± 2.8	98 ± 1.8	18.6 ± 0.3	187 ± 9.4
	All-*trans*-retinol	NC			
K212R	All-*trans*-retinal	133 ± 0.9	78 ± 3.4	13.2 ± 0.2	166 ± 3.7
	All-*trans*-retinol	NC			
Q270A	All-*trans*-retinal	176 ± 1.0	76 ± 0.8	6.0 ± 0.1	78 ± 4.2
	All-*trans*-retinol	NC			
Q270D	All-*trans*-retinal	211 ± 3.9	37 ± 0.1	7.3 ± 0.0	194 ± 6.7
	All-*trans*-retinol	1.5 ± 0.2			
Q270E	All-*trans*-retinal	309 ± 2.5	39 ± 2.7	21.1 ± 0.3	545 ± 1.5
	All-*trans*-retinol	23 ± 0.2	405 ± 29.2	1.8 ± 0.0	5 ± 1.1
Q270R	All-*trans*-retinal	NC			
	All-*trans*-retinol	NC			

The reactions were performed as described for Table 1.
NC, kinetic parameters are not calculated.
Data represent means of three experiments and ± represents standard deviations.

lowest ΔE_{bind} for all-*trans*-retinal among the substrates tested. The affinity of *M. tractuosa* AKR for the substrates followed the order all-*trans*-retinal > *9-cis*-retinal > benzaldehyde > acetaldehyde. The changes in the binding energy (ΔE_{bind}) calculated after substrate docking (Varnai et al., 1999) followed the same order as the enzyme affinity. The binding of larger aldehydes presented lower energy values (ΔE_{bind} was −46.85 kcal/mol for all-*trans*-retinal and −21.72 kcal/mol for 9-*cis*-retinal), whereas the binding of smaller aldehydes showed higher values (ΔE_{bind} was −2.16 kcal/mol for acetaldehyde and −17.71 kcal/mol for benzaldehyde). The binding of the larger aldehyde all-*trans*-retinal to the enzyme was more stable than that of the smaller aldehyde benzaldehyde. These results may explain that the affinity for all-*trans*-retinal was higher than benzaldehyde.

The affinity and specific activities of the retinal-reducing enzymes for all-*trans*-retinal and all-*trans*-retinol measured by HPLC are summarized in Table 3. The affinity for all-*trans*-retinal was the lowest in human retinol dehydrogenase (RDH10) followed by *M. tractuosa* AKR (Dalfo et al., 2007; Gallego et al., 2006; Kedishvili et al., 2002; Takahashi et al., 2009). The specific activity of *M. tractuosa* AKR was the highest among the enzymes. *M. tractuosa* AKR exhibited no activity for all-*trans*-retinol, whereas other retinal-reducing enzymes showed activity, indicating that *M. tractuosa* AKR is an effective enzyme for the conversion of all-*trans*-retinal to all-*trans*-retinol. All-*trans*-retinal has been produced by β-carotene 15,15′-oxygenases using β-carotene (Kim et al., 2007, 2008, 2010) and by metabolic engineered *E. coli* using the fed-batch culture of glycerol (Lee et al., 2012). Thus, *M. tractuosa* AKR can be applied to all-*trans*-retinol production from β-carotene by enzymatic reactions and its gene can be introduced into all-*trans*-retinal-producing metabolic engineered *E. coli* for all-*trans*-retinol production from glycerol by cultivation. NADPH-dependent AKR for retinol production by *in vitro* reaction is not economic. However, the cultivation of metabolic engineered *E. coli* expressing the AKR gene may be economic because this method does not require NADPH.

Table 3
Affinity and specific activities of retinal-reducing enzymes for all-*trans*-retinal and all-*trans*-retinol substrates.

Substrate	Parameter	Bf RDH1	Bf RDH2	Human RDH10	Human PSDR1	Human AKR1B10	*M. tractuosa* AKR
All-*trans*-retinal							
	K_m (μM)	8.7	8.9	570	0.5	0.6	48
	Specific activity (nmol min^{-1} mg^{-1})	0.3	2.3	1.1	18	300	320
All-*trans*-retinol							
	K_m (μM)	NR	NR	4.1	1.3	0.4	NC
	Specific activity (nmol min^{-1} mg^{-1})	NR	NR	0.06	1.6	80	ND
Reference		Dalfo et al. (2007)	Dalfo et al. (2007)	Takahashi et al. (2009)	Kedishvili et al. (2002)	Gallego et al. (2006)	This study

All-*trans*-retinal and all-*trans*-retinol were measured by HPLC.
NR, not reported; NC, not calculated; Bf, *Branchiostoma floridae*; PSDR, prostate short-chain dehydrogenase.

In this study, the biochemical properties of *M. tractuosa* AKR were characterized and this enzyme exhibited no activity for all-*trans*-retinol as distinct from other retinal-reducing enzymes. Thus, *M. tractuosa* AKR is an effective enzyme for the conversion of all-*trans*-retinal to all-*trans*-retinol, and can be applied in all-*trans*-retinol production from β-carotene and glycerol by biological processes.

Acknowledgment

This work was supported by Konkuk University in 2013.

Appendix A. Supplementary data

Supplementary material related to this article can be found, in the online version, at http://dx.doi.org/10.1016/j.jbiotec.2013.11.005.

References

Akhavan, A., Levitt, J., 2008. Assessing retinol stability in a hydroquinone 4%/retinol 0.3% cream in the presence of antioxidants and sunscreen under simulated-use conditions: a pilot study. Clin. Ther. 30, 543–547.

Al-Balas, Q., Hassan, M., Al-Oudat, B., Alzoubi, H., Mhaidat, N., Almaaytah, A., 2012. Generation of the first structure-based pharmacophore model containing a selective "zinc binding group" feature to identify potential glyoxalase-1 inhibitors. Molecules 17, 13740–13758.

Alzeer, S., Ellis, E.M., 2011. The role of aldehyde reductase AKR1A1 in the metabolism of gamma-hydroxybutyrate in 1321N1 human astrocytoma cells. Chem. Biol. Interact. 191, 303–307.

Blomhoff, R., Blomhoff, H.K., 2006. Overview of retinoid metabolism and function. J. Neurobiol. 66, 606–630.

Bohren, K.M., Bullock, B., Wermuth, B., Gabbay, K.H., 1989. The aldo-keto reductase superfamily. cDNAs and deduced amino acid sequences of human aldehyde and aldose reductases. J. Biol. Chem. 264, 9547–9551.

Cao, D., Fan, S.T., Chung, S.S., 1998. Identification and characterization of a novel human aldose reductase-like gene. J. Biol. Chem. 273, 11429–11435.

Crosas, B., Cederlund, E., Torres, D., Jornvall, H., Farres, J., Pares, X., 2001. A vertebrate aldo-keto reductase active with retinoids and ethanol. J. Biol. Chem. 276, 19132–19140.

Dalfo, D., Marques, N., Albalat, R., 2007. Analysis of the NADH-dependent retinaldehyde reductase activity of amphioxus retinol dehydrogenase enzymes enhances our understanding of the evolution of the retinol dehydrogenase family. FEBS J. 274, 3739–3752.

Duester, G., 1996. Involvement of alcohol dehydrogenase, short-chain dehydrogenase/reductase, aldehyde dehydrogenase, and cytochrome P450 in the control of retinoid signaling by activation of retinoic acid synthesis. Biochemistry 35, 12221–12227.

Duester, G., 2000. Families of retinoid dehydrogenases regulating vitamin A function: production of visual pigment and retinoic acid. Eur. J. Biochem. 267, 4315–4324.

Duester, G., Mic, F.A., Molotkov, A., 2003. Cytosolic retinoid dehydrogenases govern ubiquitous metabolism of retinol to retinaldehyde followed by tissue-specific metabolism to retinoic acid. Chem. Biol. Interact. 143-144, 201–210.

Endo, S., Matsunaga, T., Horie, K., Tajima, K., Bunai, Y., Carbone, V., El-Kabbani, O., Hara, A., 2007. Enzymatic characteristics of an aldo-keto reductase family protein (AKR1C15) and its localization in rat tissues. Arch Biochem. Biophys. 465, 136–147.

Endo, S., Matsunaga, T., Mamiya, H., Ohta, C., Soda, M., Kitade, Y., Tajima, K., Zhao, H.T., El-Kabbani, O., Hara, A., 2009. Kinetic studies of AKR1B10, human aldose reductase-like protein: endogenous substrates and inhibition by steroids. Arch. Biochem. Biophys. 487, 1–9.

Fukumoto, S., Yamauchi, N., Moriguchi, H., Hippo, Y., Watanabe, A., Shibahara, J., Taniguchi, H., Ishikawa, S., Ito, H., Yamamoto, S., Iwanari, H., Hironaka, M., Ishikawa, Y., Niki, T., Sohara, Y., Kodama, T., Nishimura, M., Fukayama, M., Dosaka-Akita, H., Aburatani, H., 2005. Overexpression of the aldo-keto reductase family protein AKR1B10 is highly correlated with smokers' non-small cell lung carcinomas. Clin. Cancer Res. 11, 1776–1785.

Gallego, O., Belyaeva, O.V., Porte, S., Ruiz, F.X., Stetsenko, A.V., Shabrova, E.V., Kostereva, N.V., Farres, J., Pares, X., Kedishvili, N.Y., 2006. Comparative functional analysis of human medium-chain dehydrogenases, short-chain dehydrogenases/reductases and aldo-keto reductases with retinoids. Biochem. J. 399, 101–109.

Grant, A.W., Steel, G., Waugh, H., Ellis, E.M., 2003. A novel aldo-keto reductase from *Escherichia coli* can increase resistance to methylglyoxal toxicity. FEMS Microbiol. Lett. 218, 93–99.

Jez, J.M., Bennett, M.J., Schlegel, B.P., Lewis, M., Penning, T.M., 1997. Comparative anatomy of the aldo-keto reductase superfamily. Biochem. J. 326 (Pt 3), 625–636.

Jia, G., Takahashi, R., Zhang, Z., Tsuji, Y., Sone, H., 2006. Aldo-keto reductase 1 family B7 is the gene induced in response to oxidative stress in the livers of Long-Evans Cinnamon rats. Int. J. Oncol. 29, 829–838.

Kavanagh, K.L., Klimacek, M., Nidetzky, B., Wilson, D.K., 2003. Structure of xylose reductase bound to NAD^+ and the basis for single and dual co-substrate specificity in family 2 aldo-keto reductases. Biochem. J. 373, 319–326.

Kedishvili, N.Y., Chumakova, O.V., Chetyrkin, S.V., Belyaeva, O.V., Lapshina, E.A., Lin, D.W., Matsumura, M., Nelson, P.S., 2002. Evidence that the human gene for prostate short-chain dehydrogenase/reductase (PSDR1) encodes a novel retinal reductase (RalR1). J. Biol. Chem. 277, 28909–28915.

Kim, N.H., Kim, Y.S., Kim, H.J., Oh, D.K., 2008. Optimized formation of detergent micelles of beta-carotene and retinal production using recombinant human beta,beta-carotene 15,15'-monooxygenase. Biotechnol Prog 24, 227–231.

Kim, Y.S., Kim, N.H., Kim, H.J., Lee, J.K., Kim, S.W., Oh, D.K., 2007. Effective production of retinal from beta-carotene using recombinant mouse beta-carotene 15,15'-monooxygenase. Appl. Microbiol. Biotechnol. 76, 1339–1345.

Kim, Y.S., Oh, D.K., 2010. Biotransformation of carotenoids to retinal by carotenoid 15,15'-oxygenase. Appl. Microbiol. Biotechnol. 88, 807–816.

Kim, Y.S., Park, C.S., Oh, D.K., 2010. Retinal production from beta-carotene by beta-carotene 15,15'-dioxygenase from an unculturable marine bacterium. Biotechnol. Lett. 32, 957–961.

Laskowski, R.A., Moss, D.S., Thornton, J.M., 1993. Main-chain bond lengths and bond angles in protein structures. J. Mol. Biol. 231, 1049–1067.

Lee, J.H., Choi, J.G., Kim, Y.S., Kim, K.R., Kim, S.W., Oh, D.K., 2012. Enhancement of retinal production by supplementing the surfactant Span 80 using metabolically engineered *Escherichia coli*. J. Biosci. Bioeng. 113, 461–466.

Marti-Renom, M.A., Stuart, A.C., Fiser, A., Sanchez, R., Melo, F., Sali, A., 2000. Comparative protein structure modeling of genes and genomes. Annu. Rev. Biophys. Biomol. Struct. 29, 291–325.

Martin, H.J., Breyer-Pfaff, U., Wsol, V., Venz, S., Block, S., Maser, E., 2006. Purification and characterization of akr1b10 from human liver: role in carbonyl reduction of xenobiotics. Drug Metab. Dispos. 34, 464–470.

McHarg, J., Kelly, S.M., Price, N.C., Cooper, A., Littlechild, J.A., 1999. Site-directed mutagenesis of proline 204 in the 'hinge' region of yeast phosphoglycerate kinase. Eur. J. Biochem. 259, 939–945.

Mercier, C., Chabardes, P., 1994. Organometallic chemistry in industrial vitamin A and vitamin E synthesis. Pure Appl. Chem. 66, 1509–1518.

Miller, J.V., Estell, D.A., Lazarus, R.A., 1987. Purification and characterization of 2,5-diketo-D-gluconate reductase from *Corynebacterium* sp. J. Biol. Chem. 262, 9016–9020.

Mindnich, R.D., Penning, T.M., 2009. Aldo-keto reductase (AKR) superfamily: genomics and annotation. Hum. Genomics 3, 362–370.

Mora, J.R., Iwata, M., von Andrian, U.H., 2008. Vitamin effects on the immune system: vitamins A and D take centre stage. Nat. Rev. Immunol. 8, 685–698.

Peralba, J.M., Cederlund, E., Crosas, B., Moreno, A., Julia, P., Martinez, S.E., Persson, B., Farr s, J., Pares, X., Jornvall, H., 1999. Structural and enzymatic properties of a gastric NADP(H)-dependent and retinal-active alcohol dehydrogenase. J. Biol. Chem. 274, 26021–26026.

Pino-Lagos, K., Guo, Y., Noelle, R.J., 2010. Retinoic acid: a key player in immunity. Biofactors 36, 430–436.

Raifen, R., Altman, Y., Zadik, Z., 1996. Vitamin A levels and growth hormone axis. Horm. Res. 46, 279–281.

Ruiz, F.X., Moro, A., Gallego, O., Ardevol, A., Rovira, C., Petrash, J.M., Pares, X., Farres, J., 2011. Human and rodent aldo-keto reductases from the AKR1B subfamily and their specificity with retinaldehyde. Chem. Biol. Interact. 191, 199–205.

Ruiz, F.X., Porte, S., Pares, X., Farres, J., 2012. Biological role of aldo-keto reductases in retinoic Acid biosynthesis and signaling. Front. Pharmacol. 3, 58.

Takahashi, Y., Moiseyev, G., Farjo, K., Ma, J.X., 2009. Characterization of key residues and membrane association domains in retinol dehydrogenase 10. Biochem. J. 419, 113–122, 111 p following 122.

Tien Le, D., Yoon, M.Y., Kim, Y.T., Choi, J.D., 2003. Roles of conserved methionine residues in tobacco acetolactate synthase. Biochem. Biophys. Res. Commun. 306, 1075–1082.

Tirado-Rives, J., Jorgensen, W.L., 2006. Contribution of conformer focusing to the uncertainty in predicting free energies for protein-ligand binding. J. Med. Chem. 49, 5880–5884.

Tsunoda, T., Takabayashi, K., 1995. Stability of all-*trans*-retinol in cream. J. Soc. Cosmet. Chem., 191–198.

Varnai, P., Richards, W.G., Lyne, P.D., 1999. Modelling the catalytic reaction in human aldose reductase. Proteins 37, 218–227.

von Lintig, J., 2012. Metabolism of carotenoids and retinoids related to vision. J. Biol. Chem. 287, 1627–1634.

Yim, S.K., Yun, S.J., Yun, C.H., 2004. A continuous spectrophotometric assay for NADPH-cytochrome P450 reductase activity using 1,1-diphenyl-2-picrylhydrazyl. J. Biochem. Mol. Biol. 37, 629–633.

Yoshida, K., Seki, S., Fujimura, M., Miwa, Y., Fujita, Y., 1995. Cloning and sequencing of a 36-kb region of the *Bacillus subtilis* genome between the gnt and iol operons. DNA Res. 2, 61–69.